



Manuscript ID: DOEBTO-UMD-9681-23-AO

*Full citation:* Othman, A., Aute, V., and Bacellar, D. “Feasibility Analysis on the Use of Retrofitted Air-Conditioners Using Thermal Energy Storage (TES) for High Ambient Temperature (HAT) Countries.” 14<sup>th</sup> IEA Heat Pump Conference (HPC 2023), Chicago, Illinois, USA, May 15 – 18, 2023

## Feasibility Analysis for the Use of Retrofitted Air-Conditioners Using Thermal Energy Storage (TES) for High Ambient Temperature (HAT) Countries

Al-Hussain Othman<sup>a</sup>, Vikrant Aute<sup>a\*</sup>, Daniel Bacellar<sup>a</sup>

<sup>a</sup>Center for Environmental Energy Engineering, Department of Mechanical Engineering, University of Maryland, 3151 Glenn L. Martin Hall Building, College Park, MD 20742, United States

---

### Abstract

In high ambient temperature (HAT) countries, summer temperatures exceed 35°C, degrading the performance of air-conditioning systems and straining power grids. In this paper, a feasibility analysis was conducted to investigate potential savings during the peak using latent Thermal Energy Storage (TES) at near room phase-change temperatures, replacing condensers, thus, minimizing temperature lifts. Weather data, building loads, and baseline air-conditioning systems data were gathered for Dubai. A transient vapor-compression model in Modelica was used to compare the COP, total power input and cooling capacity of the air-conditioner at peak hours when ambient temperatures range between 35 – 45 °C versus the TES-Phase-Change Material (PCM) melting temperatures from 22 – 28°C. The results indicate that the TES-PCM can enhance the system COP at the peak by a factor 1.4 and 2 for during for outdoor temperatures of 35 – 40°C, and 40 – 45°C, respectively. Lower melting temperature PCMs were able to reduce the required power input by 30-50%, with more savings occurring at higher temperature days. On the other hand, higher temperature PCMs enhancements were minimal especially at outdoor ambient temperatures ranging between 35 – 40°C. Improvements to the cooling capacity range from 8 – 18 % for the outdoor temperature range of 35 – 45 °C. An economic analysis was conducted to find the potential saving in utility costs for 30%, 60%, and 90% of the space cooling demands of Dubai, and find the trade-off points between utility savings and cost of PCM-TES implementation. If the peak loads are to be shifted by 6 hours daily, the percentage utility savings for the city is 18%. Using estimated costs of the PCM-TES, ranging from \$200-500/kWh, the daily load shifting hours were estimated to range from 4 hours at the lowest cost systems to 2.5 hours at the highest costs.

© HPC2023.

Selection and/or peer-review under the responsibility of the organizers of the 14<sup>th</sup> IEA Heat Pump Conference 2023.

*Keywords:* Room-temperature PCMs; High Ambient Temperature Countries; Feasibility analysis; City Cost Requirements

---

### 1. Introduction

Globally, space cooling already consumes 20% of the total electricity to buildings [1]. In high ambient temperature (HAT) countries, challenges in providing sustainable cooling arise in residential and commercial

---

\* Corresponding author. Tel.: 301-405-8726;  
E-mail address: vikrant@umd.edu.

buildings. Gulf Cooperation Council (GCC) countries are characterized as HAT given their extreme conditions during the summer as temperatures exceed 45°C during the day [2-3]. With such hot conditions, more power input is required by compressors to meet cooling demands, and reject heat to such extreme ambient heat sinks. This degrades the COP of air-conditioning equipment that can range from 10 to 30% depending on the refrigerant and cooling system installed [4-5]. Increases in power requirements, maximizes the strain on power grids, specifically during the peak, with air-conditioning being a major contributor to the power demand. For example, around 50% of the annual electricity demand in Dubai is consumed on air-conditioning [6]. With the continuous population growth and urban development, these demands will only grow, increasing carbon dioxide emissions as more powerplants will be required just to meet peak demands.

Thermal energy storage (TES) systems fitted with phase-change materials (PCMs) provide an opportunity to maximize the COP at peak conditions and shift the electrical demand on the grid during the day. There are several applications on retrofitted air-conditioning systems and buildings with PCM-TES systems. Chaivat & Kiatsiriroat [7] placed a thermal storage heat exchanger in return air duct precooling it prior to ventilation air mixing in Thailand. Using paraffin waxes that melt at around 20°C, the PCM was discharged at peak hours when the return temperatures are above 25°C, and recharged with cool air directly at the evaporator exit. Annual electrical cost savings of 9.1% were reported. Real et al. [8] connected PCM tanks to an experimental air-conditioning system through the means of secondary water loops for cooling. On the condenser side, the heat is rejected to the low-than-ambient PCM melting conditions ( $T_{melt}=27^\circ\text{C}$ ) during the peak, increasing the COP by 36%. Implementations of solar photovoltaics to power the compressor in the vapor-compression were also added along the thermal energy storage tanks [7, 8].

In many studies conducted the TES-PCM systems were incorporated into a heat pump through the means of a hydronic secondary loop [9–11], whether on the indoor or outdoor heat exchanger. With the exception of Maaraoui et al. [14], where the authors proposed an air-refrigerant-PCM heat exchanger for heat pumps for heating residential buildings. The configuration of the retrofitted heat pump is to have the PCM tank charge at off-peak hours with low heat load, and only the PCM storage discharge the heat at peak conditions. The limiting factor of this design was the lower thermal conductivity of PCMs, resulting in a large HX. On the other hand, the PCM storage tank did last up to 2 hours during the discharge period, which can contribute to improving the annual seasonal performance.

In this paper, the authors propose the inclusion of the TES-PCM storage in the vapor-compression cycle, with the storage tank is both heated (discharged) and cooled (charged) directly with a refrigerant-PCM heat exchanger. For a 17.5-kW (5-tons) R-410A air-conditioning unit, the ability of several PCMs with near-room melting temperatures ranging between 22-31°C were assessed as replacements for the condenser during the peak for Dubai, UAE. The TES-PCM storage will operate as the condenser for 4-hours during the peak. Using a commercial building prototype, building load data were obtained and a transient model on Modelica was used to predict real-time electrical loads. Using the retrofitted vapor compression cycle, the potential electric savings during the peak hours were assessed, along with their corresponding increases in COP and cooling capacities. Furthermore, the load shifting effect of re-charging the TES-PCM tanks were assessed, and city-level economic analysis was conducted.

## 2. Methodology

### 2.1. System Description

In this system, there are two configurations that are shown in Fig. 1. The first configuration (Fig. 1(a)) operation is twofold. The first is the conventional vapor compression cycle, that is running at off-peak conditions, with the TES system (represented as the thermal battery) is fully charged or charging. In this case, the air-conditioning system can provide cooling when lower building loads are there, not requiring excessive electrical demands, thus, not straining the electrical grid. The second operation of configuration 1 occurs when the PCM is partially or fully melted, the conventional cycle can be used to recharge the battery. This can typically occur when the internal load at low, or no indoor cooling is required. In the second configuration shown in Fig. 1(b), the refrigerant flow to the condenser is eliminated and the high-pressure refrigerant is directed to the thermal battery. This occurs during the peak-hours when the outdoor ambient conditions are extreme 35°C or higher, or when the system COP drops. Given that the thermal battery consists of PCM with melting temperatures that are lower in temperatures than ambient conditions, there is potential to reduce the required power input from the compressor increasing the COP during these hours.

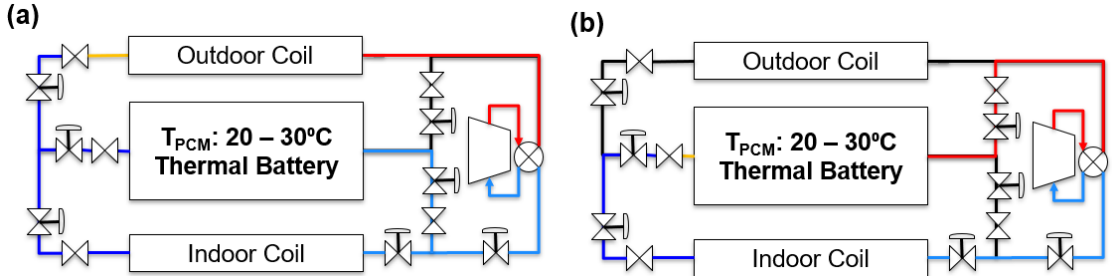


Fig. 1. Proposed cooling system (a) Configuration 1: conventional air-conditioning system for off-peak hours for fully charged or charging battery, (b) Configuration 2: thermal battery discharging cycle for on-peak hours

## 2.2. System Modeling

The TES-AC integrated cycle consisted of a variable-speed compressor, header microchannel heat exchangers for the evaporator and condenser, and an electronic expansion valve (EXV). The thermal battery model was adapted from the Modelica Standard Library [15], CEEE Modelica Library (CML) [16], Dhumane et al. [17], and Cao & Faghri [18]. The thermal battery model, was a conjugate heat transfer model, between the refrigerant and the PCM material through a material wall (CML [16]). The refrigerant heat transfer and pressure drops are already determined using the control volume available in CML [16]. The PCM transient model [17] considers the solid, two-phase and liquid region to obtain an equivalent specific heat ( $c$ ), from the enthalpy of fusion ( $H_{sl}$ ), solid ( $C_s$ ) and liquid ( $C_l$ ) specific heats. The equivalent specific heat in the mushy zone considers the average solid and liquid specific heats along with the enthalpy of fusion as per Cao & Faghri [18]. The melting range is assumed to be  $(2 \times \Delta T)$ , and  $T_m$  is the midpoint melting point in the melting range. An additional term  $s$  is a correction to the temperature difference to account for any additional changes during the melting and solidification process. Finally, the thermal energy release is predicted depending on the rate of change in enthalpy ( $dh/dt$ ), and required PCM mass (Equation (1)).

$$\begin{aligned}
 T^* &= T_{pcm} - T_m \\
 h &= c(T^* + s) \\
 c &= \begin{cases} C_s & \text{if } T^* < -\Delta T \\ \frac{C_s + C_l}{2} + \frac{H_{sl}}{2\Delta T} & \text{if } -\Delta T < T^* < \Delta T \\ C_l & \text{if } T^* > \Delta T \end{cases} \\
 s &= \begin{cases} \Delta T & \text{if } T^* < \Delta T \\ \frac{C_s}{C_l} \Delta T + \frac{H_{sl}}{C_l} & \text{if } T^* > \Delta T \end{cases} \\
 Q &= \frac{dh}{dt} M_{PCM}
 \end{aligned} \tag{1}$$

To meet the required thermal battery loads of 17.5-kW for 4 hours, the total required loads were summed for the entire time period, over the material density and enthalpy of fusion for the PCM (Equation (2)). For salt-hydrate PCMs, the material densities, range between 1.2 to 2 g/cm<sup>3</sup>, with enthalpies of fusion ranging between 100-250 kJ/kg for room temperature PCMs [19]. The reason for selecting salt hydrates as opposed to paraffin waxes, is their higher energy density [19]. To ensure that the heat transfer loads are met with PCM-TES in place, the overall UA's is in the range of 3000-5000 W/K. In this paper, the following assumptions were made:

1. The PCM-TES UA was 3000 W/K given that this is most likely the least expensive design.
2. The PCM heat transfer coefficient was assumed to be around 10 W/m<sup>2</sup>K.
3. The enthalpy of fusion was 200 kJ/kg
4. The initial PCM temperature was 15°C, with the refrigerant pressure was around 2-MPa
5. The initial conditions in the indoor coil: pressure was 1-MPa, and temperature was 9.5°C
6. The initial conditions in the outdoor coil: pressure was 2.8-MPa, and temperature was 45°C

$$V_{PCM} = \frac{\int_0^{4h} \dot{Q} dt}{\rho_{PCM} \cdot H_{sl}} \quad (2)$$

The variable speed compressor model, consists of multiple 10-coefficient maps each corresponding to a frequency level. The model switched between the maps based on the required cooling capacity from the building load. Similarly, the EXV model consists of a variable opening orifice, that is adjusted by the manufacturers pulse-capacity curves and degrees of superheat. The dimensions and properties of the microchannel evaporator and condenser were inputted in the CML [16] MCHX models.

Each configuration in Fig. 1 was modeled in a separate cycle, and the cycles were operating based on the required air mass flow rates for the evaporator (indoor coil) and condenser side (outdoor coil) (Fig. 2). When the required cycles are off, the indoor and outdoor mass flow rates are set to near-zero amounts, according to a time schedule set by the building loads. During the day, the indoor mass flow rates are included based on the corresponding building load, and the outdoor mass flow rate is determined by the manufacturers fan curves at the operating conditions. The remaining outdoor and indoor boundary conditions (temperatures and humidity ratios), were obtained from the weather data sets [20] and prototype commercial building models [21], respectively. When the thermal battery is discharging during peak hours, the only boundary conditions to the cycle are the indoor air temperature, humidity and mass flow rate (Fig. 3(a)), and during the charging stage the outdoor weather data, along with the operating air mass flow rate are the only boundary conditions (Fig. 3(b)). The prototype building model, in EnergyPlus [22], consists of a small office building with 4 office rooms and one corridor, with building loads around 15-18 kW. Using this building prototype EnergyPlus files [21-22] for Dubai along with the locations corresponding weather data, the required boundary conditions were obtained on the indoor coil of the Modelica model.

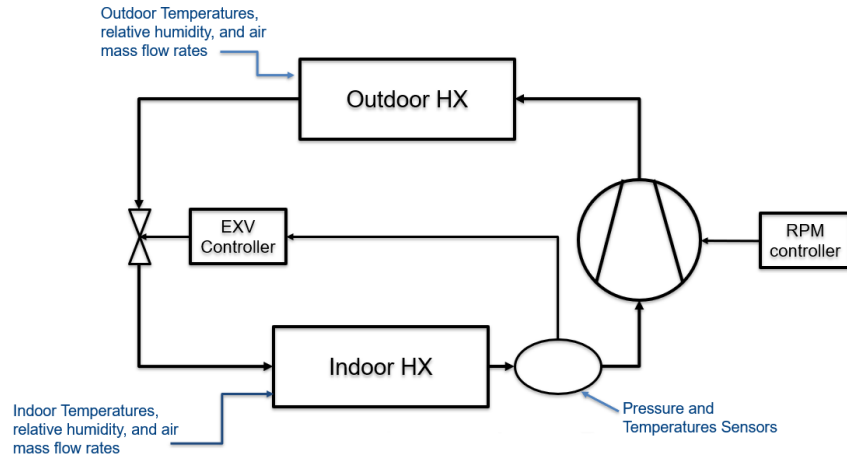


Fig. 2: Conventional air-conditioning model

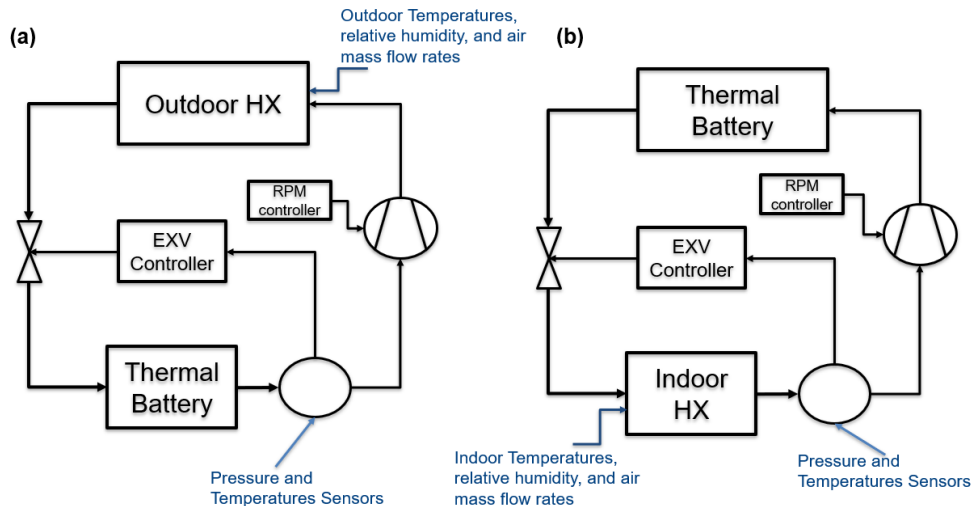


Fig. 3: Thermal battery cycle in (a) discharging mode during the peak, and (b) recharging mode during off-peak conditions

### 2.3. Selection of Days and PCM Melting Temperatures

For the summer months, between May and September, the weather data [20] obtained was analysed to see the peak temperatures per day. From Fig. 4, the peak temperatures can be divided into two ranges: 35-40°C and 40-45°C. While there are other impacts on the building cooling demands, including indoor thermal demands, and outdoor humidity and incoming sun radiation, in this paper, the focus will be more towards the outdoor temperature, as the sole objective of the PCM-TES is to lower the temperature/and pressure lift in the air-conditioning cycle, thus reducing the compressor power during the peak. Three days were selected for each peak range.

In this study, three mid-point melting temperatures were selected (a) 22°C, (b) 25°C, and (c) 28°C. The outputs from each day was averaged for its corresponding peak temperature. According to the Government of Dubai, the peak hours occur between 12:00 PM and 6:00 PM during the summer [23]. As the first step, the conventional air-conditioning model (Fig. 2) to assess the COPs during the 6-hour peak period. Based on the lowest COPs for these 6-hours, a 4-hour period was selected, and the thermal battery discharging model operation times were set (Fig. 3). Having the TES operate for 4-hour rather than the complete 6-hour period is due to the excessive mass of the TES system. As mention in section 2.2, enthalpies of fusion ranging between 100-250 kJ/kg, the mass of the PCM can range from 1,000-1,200 kg at 4-hours to at 1800-2,000-kg at 6-hours. That increase in mass can pose installation challenges along with the current lack of economic benefits over the entire 6-hours shown in Section 3.3.

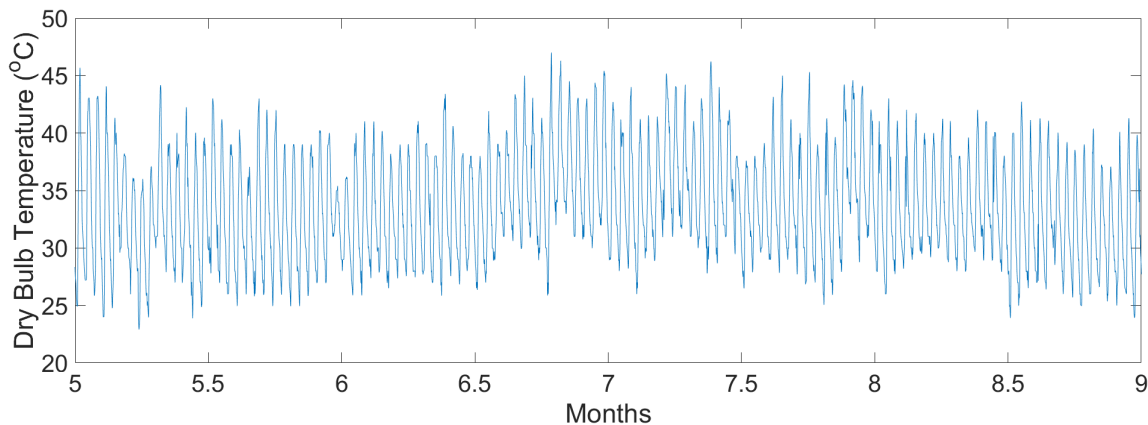


Fig. 4: Temperature Profile for Dubai, UAE

## 3. Results and Discussion

### 3.1. Effect of the PCM temperatures on the conventional system

For a day with the peak temperatures ranging between 35-40°C (Fig. 5a), it can be seen that near room PCM temperatures have provided a significant increase in COP at the peak, from 15% at  $T_{PCM} = 28^\circ\text{C}$  to 51% at  $T_{PCM} = 22^\circ\text{C}$ . However, the improvements in COP for higher ambient temperature days (40-45°C) are significantly higher, shown in Fig. 5(b), with factors ranging from 1.6 to 2 of original system when the PCM melting temperatures are 28°C and 22°C, respectively. This increase in COP can provide an excellent opportunity to reduce the strain on the grid and provide a higher cooling capacity, especially during the peak hours at high ambient temperatures.

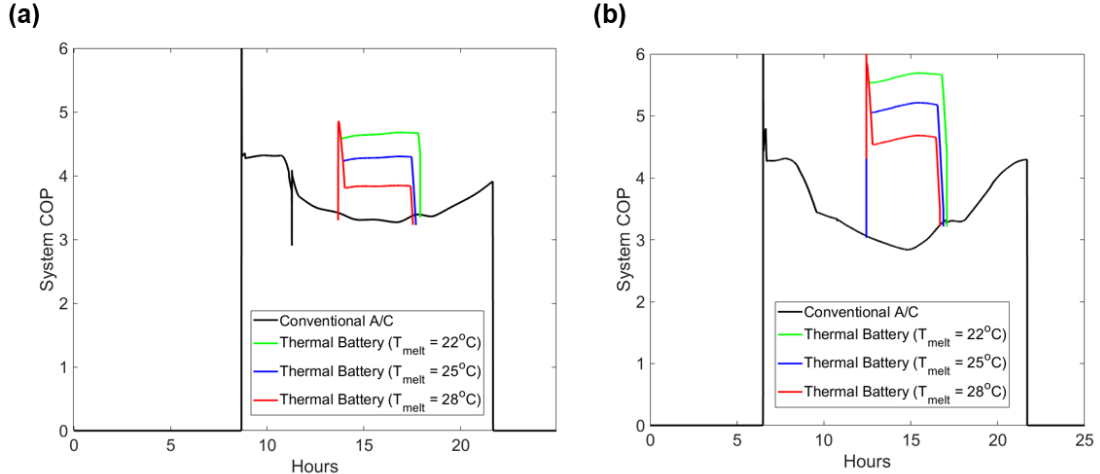


Fig. 5: Improvement in system COP for during the peak hours resulting from the thermal battery for PCM melting temperatures ranging from 22 – 28°C during the peak, when daily maximum outdoor temperatures are between (a) 35 – 40°C and (b) 40 – 45°C

Fig. 6 compares the reduction in the total power demand required by the air-conditioner for the two ambient temperature ranges. This power demand is the total compressor power input from the grid with the outdoor and indoor fans. In Fig. 6(a), the power demand increases from 9 to 11 a.m., given the increase of the building load, therefore increasing the compressor power. Given that at higher outdoor temperatures, the compressor requires higher power input to accommodate the required temperature and pressure lifts just to meet the required cooling demands. As of such, the reduction in the total power during the peak hours (Fig. 6(b)) are significantly higher when the temperatures are 40-45°C compared to the lower ambient temperature cases. Furthermore, the reduction in the total is lower with the melting temperatures are higher. Another benefit of the retrofitted PCM-TES, is the elimination of the outdoor fan, therefore, eliminating the fan power consumed during the peak. Table 2 shows the percentage savings for each PCM melting temperature. For the higher ambient temperatures, one can see that the potential for power consumption during the peak is between 30 – 45 % of the conventional A/C system. This can be beneficial to high ambient temperature countries, given that such reductions can potentially eliminate plans of building more powerplants, just to meet the electrical loads during the peak hours.

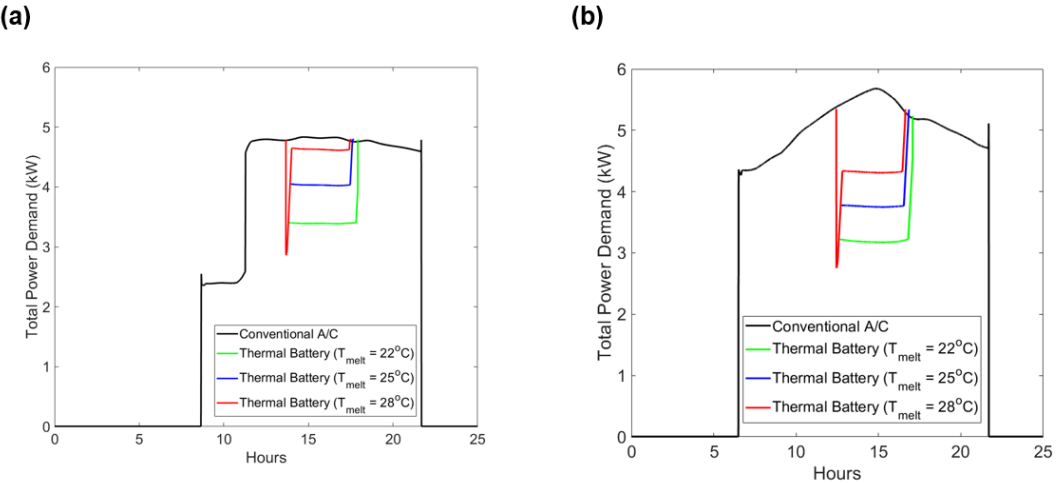


Fig. 6: Reduction in the power demand from the compressor and fans during the peak when the maximum daily outdoor temperatures are between (a) 35 – 40°C, and (b) 40 – 45°C

Another reason for the COP improvements during the peak hours for the retrofitted cycle was the increase in the cooling capacity of the system (Table 1). The cooling capacity of the system ranges from 17-18.5 kW. This occurs as the pressure lift decreases, and the PCM thermal battery dissipating almost the same amount of heat as the condenser at a lower pressure, the refrigerant is entering the evaporator at a lower vapor mass fraction (0.15-0.19) than the conventional system (0.22). This has resulted in increases in the cooling capacity ranging from 8% to 18%. The highest increases in the cooling capacity occurs during the with the PCM melting temperature being 22°C, given that at these conditions the lowest pressure and temperature lifts are obtained.

Furthermore, the percentage increase in outdoor temperature ranges of 40 – 45°C, given that the pressure and temperature lift drops are the higher in these cases as compared to the 35 – 40°C peak outdoor ambient temperatures. Therefore, the inclusion of thermal battery can provide another advantage as there is a lower need to oversize the air-conditioning system, especially at the summer peak conditions which can in turn have potential savings on the electrical grid.

Table 1. Maximum percentage changes in COP, power consumption and cooling capacities for the different PCM melting temperatures at different ambient conditions during the peak hours

PCM melting temperature	22°C	25°C	28°C
% increase in COP $T_{amb} = 35 - 40°C$	42.5	31.2	17.4
% increase in COP $T_{amb} = 40 - 45°C$	99.6	82.5	63.5
% power savings for $T_{amb} = 35 - 40°C$	30.2	17.1	4.9
% power savings for $T_{amb} = 40 - 45°C$	51.2	33.1	24.4
% increase in cooling capacity $T_{amb} = 35 - 40°C$	10.1	9.8	8.7
% increase in cooling capacity $T_{amb} = 40 - 45°C$	18.1	14.8	12.5

### 3.2. Energy Required for Load Shifting

In this section, an assessment of the electrical load required to recharge or (solidify) the thermal battery during nighttime was conducted. This is important to quantify the estimated saving during the peak to the energy required to recharge the battery. Table 2 shows the required power consumption by the air-conditioning system in kWh. The reduction in power input with higher PCM melting temperatures is due to the lower temperature difference between them and the outdoor ambient temperatures which are typically between 25°C and 30°C, along with the minor reduction in charging time between the different temperature PCMs (<400 seconds). The selection of PCM appropriate melting temperature relies mostly on the available savings that can be achieved during the peak, without have excessive recharge costs. While the cooling capacity for the three PCMs are close (17-17.5 kW), the choice of the PCM temperature effects mostly how much can be alleviated from the grid during the peak, without excessive energy when recharging. Looking at the saving of the PCM melting at 22°C, the savings along with the recharge power, it is acceptable to recharge that PCM with this power.

Table 2. Power required in kWh for the thermal battery during night-time for different PCM melting temperatures

PCM Melting Temperature (°C)	Total Power Input required (kW)	Time required for full recharge (hours)	COP for Cycle Recharge
22	3.81	4.7	4.15
25	3.67	4.5	4.45
28	3.45	4.4	4.65

### 3.3. Economic Analysis

An economic analysis was conducted to assess to the potential savings for Dubai during the peak hours. This analysis can help predicting the expected savings from increases in meeting the city building more powerplants, just to meet the required cooling demands. According to the Dubai Electricity and Water Authority (DEWA), the peak electrical demand in 2021 was 9,204 MW occurring in August, when the outdoor ambient temperatures exceed 40°C. So far, the city of Dubai can generate 13,417 MW, with 89% of the power is generated through steam and gas turbines, and 11% is generated by solar photovoltaics [23].

Currently, air-conditioning is responsible for 50% of all the electricity consumed [6]. The thermal battery will consist of the PCM material and heat exchangers. However, even with the low cost PCM (\$3-30/kWh [19]), current commercially available thermal battery technologies put their cost between \$200-500/kWh [24], given heat exchanger material cost and assembly requirements. In this analysis, the objective was to identify the number of hours for the thermal battery to operate during the peak that can be used to reduce the demand

cost for 30%, 60%, and 90% of the city, against the amount the estimated city cost of the thermal battery to meet that required demands.

Table 3: Current Dubai power station capacities [25]

Power Stations	Power Station Type	Current Energy Production Year 2021 (MW) [25]
Aweer Power Station "H" Phases I to III	Natural Gas and Diesel Turbines	1996
Hassyan Power Plant Phases I and II	Natural Gas Turbines (Converted from Coal)	1200
Jebel Ali Station "D"		1027
Jebel Ali Station "E"		616
Jebel Ali Station "G"	Natural gas and oil combined cycle	818
Jebel Ali Station "K"		948
Jebel Ali Station "L" Phases I to II		2401
Jebel Ali Station "M" with Extension		2885
Mohammed bin Rashid Al Maktoum "All Phases until 2022"	Currently Solar PV	1526

Dubai has several powerplants (Table 3), with investments up to 6.6 Billion USD [26]–[29]. During the peak, it is assumed that all the powerplants are operating at full capacity, bringing the estimated cost during the peak at \$0.49/kWh. According to DEWA [23], Dubai has a single utility rate per kWh, depending on the amount of electricity consumed per month. Fig. 7, and Fig. 8, shows the estimated cost savings for 30%, 60%, and 90% of the city using the electrical space cooling demands of 2021.

For a PCM with a melting temperature of 22°C, Table 1 provides us with potential energy savings of a retrofitted air-conditioner with TES at two maximum outdoor temperature ranges. Using the meteorological data in TMY3, it was observed that on average during the summer the outdoor temperature exceeds 40°C for one hour during the day. For limited operation, the energy savings were calculated for this one-hour using the corresponding percentage reduction of 51%. For longer operating periods the total savings were calculated by a weighted average corresponding to the number of hours per year in the different temperature ranges. From this, we obtain the overall utility reduction estimate of 18% for the entire 6 hours, shown in Figs. 7 and 8. This brings the total savings electricity costs to \$0.59 and \$1.78 billion for 30% to 90% of Dubai's space cooling demand reduction, respectively. That percentage saving is due to the single utility rate per kWh used, rather than having variable rate depending on the peak hours or non-peak hours. In all scenarios, 30% to 90%, the are annual cost savings that increase with more peak hour loads alleviated by the TES, that corresponds to electrical savings at the peak.

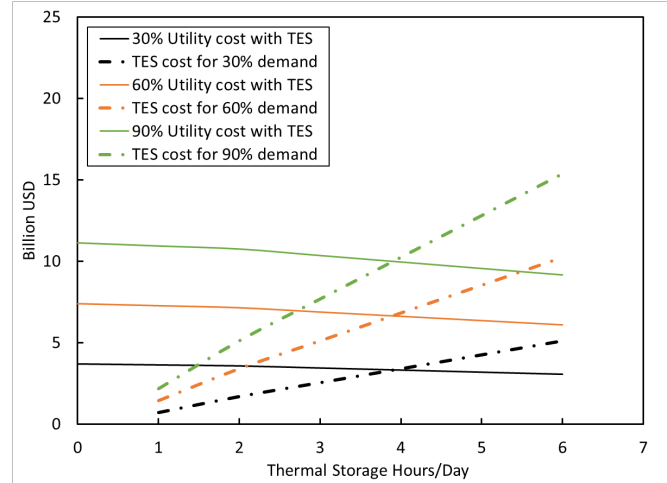


Fig. 7: Predict savings in the utility cost when using TES at against cost of \$200/kWh of thermal energy storage per operating hours daily for 30%-90% of the AC requirements

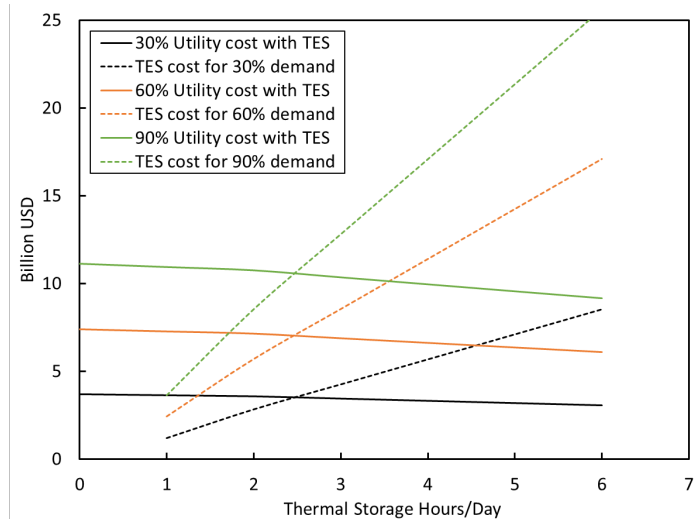


Fig. 8: Predict savings in the utility cost when using TES at against cost of \$500/kWh of thermal energy storage per operating hours daily for 30%-90% of the AC requirements

The key challenge is to identify the point which is the trade-off between the cost of the PCM-TES and the number of hours the can be altered. Thus, the cost of TES/kWh is an important factor, and that lower cost TES systems are required, to increase the number of hours that can be used to load shift. For the lower bound of \$200/kWh, it is logical to provide TES for 4 hours during the peak, which is the assumed number of TES hours in this study. More hours, will result in higher investment costs than the potential savings. At the higher cost of TES rates, the number of peak load hours shift will reduce to 2.4 hours and if an investment is done at this cost, the operation of TES should only be there at the highest temperature hours of the year. If a cost of \$15/kWh of TES is achieved [30] the city of Dubai can provide TES for the entire 6-hour peak for 90% of its citizens at a \$1.1 billion, giving a payback period of 2 years only, and not 10 years (TES cost \$200/kWh).

### 3.4. Challenges with the retrofitted TES-PCM air-conditioning system

While the cost of PCM materials are quite low, there still remains challenges in designing and assembling a TES, especially for large applications. This is due to PCMs being constrained by their material properties. PCMs have low thermal conductivities, and a finite energy storage ( $\sim 100 - 250 \text{ kJ/kg}$  for salt hydrates) [19]. To get more thermal energy stored, more PCM is needed, however, the compactness of the TES system must not be affected, not to degrade the heat transfer. Increasing the PCM volumes and heat transfer surface areas, will result in increasing the internal volumes on the refrigerant side, therefore increasing refrigerant charge in the cycle, which is problematic for higher-GWP refrigerants and flammable alternatives. All these challenges

can drive the cost of TES systems to increase. Nonetheless, with more research in the design, assembly, and demand for enhanced PCM-TES systems, the cost will start to decrease.

Retrofitting the air-conditioning system with the TES storage has several challenges. Firstly, if the available system has a single-speed compressor, designed for higher temperature lifts, reducing that temperature lift with the TES can potentially degrade the isentropic efficiency of that compressor, degrading the potential savings that can be achieved during the peak. Thus, a variable speed compressor may be used to operate at lower compressor RPMs to meet the building loads at lower temperature lifts, without degrading the isentropic efficiency. Secondly, explicit controls are required to ensure that the cycle can achieve a set point superheat and subcooling when operating with the TES, as lower the pressure and temperature lifts presents hurdles on both the condenser and evaporator obtaining subcooling and superheating. Finally, the air-conditioning refrigerant cycle will require a number of on/off valves to switch refrigerant flows between the outdoor condenser and the TES during peak hours, along with adequate controls to ensure that this switch can occur smoothly, without damaging any cycle component.

#### 4. Conclusions

In this paper, a proposed retrofitted air-conditioning system with near to room temperatures PCM-TES feasibility was investigated for a city in a HAT country (Dubai). A transient model in Modelica was built and used to assess the potential power savings during the peak for a 17.5-kW R-410A air-conditioning unit, and the electrical loads required to recharge the PCM-TES. Using the typical meteorological year data, two types of days were analyzed, days with peak temperatures ranging between 35 – 40°C, and others with peak temperatures above 40°C. For each outdoor temperature ranges, the COP, total power input and cooling capacity was assessed. For higher ambient temperature days, a PCM-melting point of 22°C, can result in COPs almost doubling, reduction in the power consumption during the peak by up to 50%, and increases in cooling capacities by 18% during the peak hours. As the PCM melting temperatures increase, the enhancements to the cycle during the peak hours reduces, especially when outdoor temperatures are below 40°C. From an economic standpoint, given the higher costs of PCM-TES/kWh, the number of hours for feasible application of PCMs can range between 2.5-hours per day (\$500/kWh), to 4-hours a day (\$200/kWh) for an entire year with capital investments ranging from \$4 – 12 billion depending on the range of the city cooling load to be met (30% – 90%). With more research in the design and assembly of PCM-TES, its cost can further drop, reducing the capital investments into the system to a fraction of the current costs.

#### Acknowledgements

This material is based upon work supported by the U.S. Department of Energy's Office of Energy Efficiency and Renewable Energy (EERE) under the Building Technologies Office Award Number DE-EE0009681. The views expressed herein do not necessarily represent the views of the U.S. Department of Energy or the United States Government. This work was also funded in part by the Modeling and Optimization Consortium at the University of Maryland.

#### References

- [1] IEA, "The Future of Cooling –Opportunities for energy-efficient air conditioning," International Energy Agency (IEA), 2018. Accessed: Jun. 10, 2022. [Online]. Available: <https://www.iea.org/reports/the-future-of-cooling>
- [2] M. Haddad, "Mapping the hottest temperatures around the world." <https://www.aljazeera.com/news/2021/7/1/interactive-mapping-hottest-temperatures-around-world> (accessed Jun. 10, 2022).
- [3] NASA Earth Observatory, "Land Surface Temperature," Mar. 31, 2022. [https://earthobservatory.nasa.gov/global-maps/MOD\\_LSTD\\_M](https://earthobservatory.nasa.gov/global-maps/MOD_LSTD_M) (accessed Jun. 10, 2022).
- [4] M. A. Ansari, T. Hussain, S. A. Khan, S. Mustafa, and V. Goyal, "Experimental investigation on VCRS by using R-134a and R-410a of air and evaporative cooled condenser," *IOP Conf. Ser. Mater. Sci. Eng.*, vol. 691, no. 1, p. 012071, Nov. 2019, doi: 10.1088/1757-899X/691/1/012071.
- [5] R. Bruno, F. Nicoletti, G. Cuconati, S. Perrella, and D. Cirone, "Performance Indexes of an Air-Water Heat Pump Versus the Capacity Ratio: Analysis by Means of Experimental Data," *Energies*, vol. 13, no. 13, Art. no. 13, Jan. 2020, doi: 10.3390/en13133391.

- [6] “Dubai Demand Side Management (DSM) –2016 Annual Report ‘For an Efficient Cooling,’” Dubai Supreme Council of Energy, Dubai. Accessed: Nov. 09, 2022. [Online]. Available: <https://dubaisce.gov.ae/en/taqati/>
- [7] N. Chaiyat and T. Kiatsiriroat, “Energy reduction of building air-conditioner with phase change material in Thailand,” *Case Stud. Therm. Eng.*, vol. 4, pp. 175–186, Nov. 2014, doi: 10.1016/j.csite.2014.09.006.
- [8] A. Real, V. García, L. Domenech, J. Renau, N. Montés, and F. Sánchez, “Improvement of a heat pump based HVAC system with PCM thermal storage for cold accumulation and heat dissipation,” *Energy Build.*, vol. 83, pp. 108–116, Nov. 2014, doi: 10.1016/j.enbuild.2014.04.029.
- [9] Y. Xu and M. Li, “Impact of instantaneous solar irradiance on refrigeration characteristics of household PCM storage air conditioning directly driven by distributed photovoltaic energy,” *Energy Sci. Eng.*, vol. 10, no. 3, pp. 752–771, 2022, doi: 10.1002/ese3.1050.
- [10] M. Fiorentini, P. Cooper, and Z. Ma, “Development and optimization of an innovative HVAC system with integrated PVT and PCM thermal storage for a net-zero energy retrofitted house,” *Energy Build.*, vol. 94, pp. 21–32, May 2015, doi: 10.1016/j.enbuild.2015.02.018.
- [11] R. Hirmiz, H. M. Teamah, M. F. Lightstone, and J. S. Cotton, “Performance of heat pump integrated phase change material thermal storage for electric load shifting in building demand side management,” *Energy Build.*, vol. 190, pp. 103–118, May 2019, doi: 10.1016/j.enbuild.2019.02.026.
- [12] Q. Meng, Y. Xi, X. Ren, H. Li, L. Jiang, and L. Yang, “Thermal Energy Storage Air-conditioning Demand Response Control Using Elman Neural Network Prediction Model,” *Sustain. Cities Soc.*, vol. 76, p. 103480, Jan. 2022, doi: 10.1016/j.scs.2021.103480.
- [13] B. D. Mselle, G. Zsembinszki, D. Vérez, E. Borri, and L. F. Cabeza, “A detailed energy analysis of a novel evaporator with latent thermal energy storage ability,” *Appl. Therm. Eng.*, vol. 201, p. 117844, Jan. 2022, doi: 10.1016/j.applthermaleng.2021.117844.
- [14] S. Maaraoui, D. Clodic, and P. Dalicieux, “Heat Pump With a Condenser Including Solid-Liquid Phase Change Material,” *Int. Refrig. Air Cond. Conf.*, Jan. 2012, [Online]. Available: <https://docs.lib.purdue.edu/iracc/1194>
- [15] “Modelica Documentation.” <https://doc.modelica.org/> (accessed Oct. 12, 2022).
- [16] H. Qiao, V. Aute, and R. Radermacher, “Transient modeling of a flash tank vapor injection heat pump system – Part I: Model development,” *Int. J. Refrig.*, vol. 49, pp. 169–182, 2015, doi: <https://doi.org/10.1016/j.ijrefrig.2014.06.019>.
- [17] R. Dhumane, J. Ling, V. Aute, and R. Radermacher, “Dynamic Modeling of a Personal Cooling Device with PCM Storage,” in *Proceedings of 12th IEA Heat Pump Conference*.
- [18] Y. Cao and A. Faghri, “A Numerical Analysis of Phase-Change Problems Including Natural Convection,” *J. Heat Transf.*, vol. 112, no. 3, pp. 812–816, Aug. 1990, doi: 10.1115/1.2910466.
- [19] J. Hirshey, K. R. Gluesenkamp, A. Mallow, and S. Graham, “Review of Inorganic Salt Hydrates with Phase Change Temperature in Range of 5 to 60°C and Material Cost Comparison with Common Waxes,” *Int. High Perform. Build. Conf.*, Jul. 2018, [Online]. Available: <https://docs.lib.purdue.edu/ihpbc/320>
- [20] “EnergyPlus.” <https://energyplus.net/weather> (accessed Nov. 03, 2022).
- [21] “Prototype Building Models | Building Energy Codes Program.” <https://www.energycodes.gov/prototype-building-models> (accessed Nov. 03, 2022).
- [22] “EnergyPlus.” <https://energyplus.net/> (accessed Nov. 14, 2022).
- [23] “Dubai Electricity & Water Authority | Peak Load.” <https://www.dewa.gov.ae/en/about-us/sustainability/lets-make-this-summer-green/peak-load> (accessed Nov. 07, 2022).
- [24] “Sunamp UniQ eHW Heat Battery - Solar and Heat Store,” Jul. 12, 2021. <https://solarandheatstore.com/product/sunamp-uniq-ehw-heat-battery/> (accessed Nov. 10, 2022).
- [25] “Annual Statistics 2021,” Dubai Electricity and Water Authority (DEWA), Dubai, UAE, 2021. Accessed: Nov. 09, 2022. [Online]. Available: <https://www.dewa.gov.ae/en/about-us/strategy-excellence/annual-statistics>
- [26] “DEWA Completes 84.52% Construction On Phase 4 Of H-Station In Al Aweer - MEP Middle East,” Jul. 08, 2021. <https://www.mepmiddleeast.com/projects/78681-dewa-completes-8452-construction-on-phase-4-of-h-station-in-al-aweer> (accessed Nov. 09, 2022).
- [27] “Work on UAE’s Mohammed bin Rashid Al Maktoum Solar Park is progressing as per schedule.” <https://www.zawya.com/en/business/energy/work-on-uaes-mohammed-bin-rashid-al-maktoum-solar-park-is-progressing-as-per-schedule-n5q9dr68> (accessed Nov. 09, 2022).
- [28] “Jebel Ali M-Station,” *Power Technology*. <https://www.power-technology.com/projects/jebel-ali-m-station/> (accessed Nov. 09, 2022).
- [29] “Al Aweer Gas Turbine Power Station ‘H.’” <https://www.besix.com/en/projects/alaweer gasturbinepowerstationh> (accessed Nov. 09, 2022).
- [30] “Thermal Energy Storage,” *Energy.gov*. <https://www.energy.gov/eere/buildings/thermal-energy-storage>

(accessed Nov. 10, 2022).